

Efficiently Solving Spin-Boson Dynamics Via Non-Markovian Quantum Trajectories

Zeng-Zhao Li,^{1,2,*} Cho-Tung Yip,^{2,*} Hai-Yao Deng,^{2,3} Mi Chen,⁴ Ting Yu,^{1,5} J. Q. You,¹ and Chi-Hang Lam²

¹*Beijing Computational Science Research Center, Beijing 100084, China*

²*Department of Applied Physics, Hong Kong Polytechnic University, Hung Hom, Hong Kong, China*

³*International Center for Materials Nanoarchitectonics,
National Institute for Materials Science, Namiki 1-1, Tsukuba 305-0044, Japan*

⁴*Department of Physics, Fudan University, Shanghai 200433, China*

⁵*Center for Controlled Quantum Systems and Department of Physics and Engineering Physics,
Stevens Institute of Technology, Hoboken, New Jersey 07030, USA*

(Dated: March 31, 2022)

We develop a systematic and efficient approach for numerically solving the non-Markovian quantum state diffusion equations for open quantum systems coupled to an environment up to arbitrary orders of noises or coupling strengths. As an important application, we consider a real-time simulation of a spin-boson model in a strong coupling regime that is difficult to deal with using conventional methods. We show that the non-Markovian stochastic Schrödinger equation can be efficiently implemented as a real-time simulation for this model, so as to give an accurate description of spin-boson dynamics beyond the rotating-wave approximation.

Dynamics of open quantum systems has been extensively studied in the last decades due to its pivotal importance in the areas of quantum optics, quantum dissipative dynamics and quantum information [1–3]. The Lindblad master equations under the Born-Markov approximations are the major theoretical tools in depicting quantum evolution under the influence of external noises, but they are doomed to fail when the system-environment coupling becomes strong or when the environment is a structured medium [3, 4]. Moreover, the widely used rotating-wave approximation (RWA) ceases to be valid at a strong coupling regime as shown by the recent experimental realization of strong and ultrastrong couplings [2, 5, 6]. It becomes clear that to correctly explain the novel quantum-mechanical phenomena arising from the strong-coupling physics, the counter-rotating terms neglected in the RWA must be taken into account properly. In addition, the counter-rotating terms are known to be important in understanding quantum Zeno and anti-Zeno effects [7–9]. All the current researches going beyond the RWA and Markov approximation have shown the necessity of developing a powerful approach to dealing with new physics arising from the strong coupling between the open quantum system of interest and its environments [8–12].

A stochastic Schrödinger equation named the non-Markovian quantum state diffusion (QSD) equation derived from a microscopic model has several advantages over the exact master equations. While the exact master equations exist only for a few solvable models [2, 13], the exact QSD equation has been established for a generic class of quantum open systems [14–16]. However, the applications of the exact QSD equation are severely limited unless this time-nolocal integro-differential equation can be cast into a numerically implementable time-local form [15–20]. In the real-world problems, solving the exact dynamical equations in a strong coupling regime is

very difficult. Therefore, it is imperative to develop an efficient perturbative method that can be implemented to solve open system dynamics dictated by the strong coupling and structured medium.

In this letter, we develop a systematic and efficient approach to solving the non-Markovian QSD equations for open quantum systems up to arbitrary orders of noises or coupling strengths. The major breakthrough is to convert the non-Markovian QSD equation into a set of coupled stochastic ordinary differential equations (SODE's) which efficiently evaluates a series expansion of the previously unsolvable O -operator up to arbitrarily high orders. The method can be generally applied to an arbitrary finite-state open system coupled to a bosonic bath. As an important example, our method is used to solve a spin-boson model with a Lorentzian environment at zero temperature in the strong coupling regime that is previously intractable when real-time quantum dynamics is needed.

Exact QSD equation. – To put our discussion into perspective, we first consider a generic open quantum system with the following Hamiltonian (setting $\hbar = 1$) [15]:

$$H_{\text{tot}} = H_{\text{sys}} + \sum_k (g_k L b_k^\dagger + g_k^* L^\dagger b_k) + \sum_k \omega_k b_k^\dagger b_k, \quad (1)$$

where H_{sys} is the system's Hamiltonian, L is the Lindblad operator, and b_k denotes the annihilation operator of the k th mode of the bosonic bath. The state of the bath may be specified by a set of complex numbers $\{z_k\}$ labeling the coherent states of all modes. The function z_t that characterizes time-dependent states of the bath may be defined by the Fourier expansion $z_t^* \equiv -i \sum_k g_k^* z_k^* e^{i\omega_k t}$. When z_k is interpreted as a Gaussian random variable, then z_t becomes a Gaussian process with the correlation function obtained by the statistical mean $\alpha(t-s) = \langle z_t z_s^* \rangle = \sum_k |g_k|^2 e^{-i\omega_k(t-s)}$. For the simple case with a zero-temperature bath, the system state at time t obeys

tained from projecting the total state to the bath state $|z\rangle$, $\psi_t(z^*) \equiv \langle z|\Psi_{\text{tot}}(t)\rangle$, which is called a quantum trajectory, obeys a linear QSD equation [14]

$$\dot{\psi}_t = -iH_{\text{sys}}\psi_t + Lz_t^*\psi_t - L^\dagger\bar{O}(t, z^*)\psi_t. \quad (2)$$

Here, the O -operator is defined by $\delta\psi_t/\delta z_s^* = O(t, s, z^*)\psi_t$, and $\bar{O}(t, z^*) = \int_0^t \alpha(t-s)O(t, s, z^*)ds$. Evaluating the O operator poses a major challenge in solving quantum open systems in real world applications. It is remarkable that the evolution is completely decoupled from projections to other bath states and hence can be solved independently. In practice, one may adopt an importance sampling scheme in which the normalized system state $\tilde{\psi}_t(z^*) = \psi_t(z^*)/|\psi_t(z^*)|$ is governed by the norm-conserving nonlinear QSD equation [14],

$$\begin{aligned} \dot{\tilde{\psi}}_t &= -iH_{\text{sys}}\tilde{\psi}_t + (L - \langle L \rangle_t)\tilde{z}_t^*\tilde{\psi}_t \\ &\quad - [(L^\dagger - \langle L^\dagger \rangle_t)\bar{O} - \langle (L^\dagger - \langle L^\dagger \rangle_t)\bar{O} \rangle_t]\tilde{\psi}_t, \end{aligned} \quad (3)$$

where \bar{O} denotes $\bar{O}(t, z^*)$ and $\langle \dots \rangle_t = \langle \tilde{\psi}_t | \dots | \tilde{\psi}_t \rangle$. We define a shifted noise as $\tilde{z}_t^* = z_t^* + y_t$, where the shift $y_t = \int_0^t \alpha^*(t, s)\langle L^\dagger \rangle_s ds$ satisfies $y_0 = 0$, and

$$\dot{y}_t = -\gamma y_t + \alpha^*(0)\langle L^\dagger \rangle_t. \quad (4)$$

The state of the open quantum system at t , represented by the reduced density matrix $\rho_t = \text{Tr}_{\text{env}}|\Psi_{\text{tot}}\rangle\langle\Psi_{\text{tot}}|$, can be recovered from an ensemble average $\rho_t = \langle |\tilde{\psi}_t(z^*)\rangle\langle\tilde{\psi}_t(z^*)| \rangle$.

The QSD equations (2) and (3) are exact. A key challenge is the determination of the O operator contained in these equations. For most practical problems except for a few specific examples where the exact O may be explicitly determined [15–20], one has to resort to a functional expansion [17] in terms of \tilde{z}_t^* which after adapting to \bar{O} writes,

$$\begin{aligned} \bar{O}(t, z^*) &= \bar{O}^{(0)}(t) + \int_0^t \bar{O}^{(1)}(t, v_1)\tilde{z}_{v_1}^* dv_1 \\ &\quad + \int_0^t \int_0^t \bar{O}^{(2)}(t, v_1, v_2)\tilde{z}_{v_1}^*\tilde{z}_{v_2}^* dv_1 dv_2 + \dots \\ &\quad + \int_0^t \dots \int_0^t \bar{O}^{(n)}(t, v_1, \dots, v_n)\tilde{z}_{v_1}^* \dots \tilde{z}_{v_n}^* \\ &\quad \times dv_1 \dots dv_n + \dots, \end{aligned} \quad (5)$$

where $\bar{O}^{(n)}$ is symmetric with respect to the time variables v_i . However, finding $\bar{O}^{(n)}$ and performing the integrations for higher order terms are formidable tasks and

have only been performed up to $n \leq 2$ for some specific models [21].

SODE formulation. – In this work, we show that the QSD perturbation may be carried out to an arbitrary order of noise terms. Specifically, we can efficiently evaluate Eq. (5) up to $\mathcal{N} = 100$ perturbative terms for the spin-boson model under consideration. We first rewrite it as

$$\bar{O}(t, z^*) = \sum_{n=0}^{N_Q} Q_0^{(n)}(t, z^*), \quad (6)$$

where $N_Q = \mathcal{N}$ nominally but we allow $N_Q < \mathcal{N}$ when higher order terms are vanishingly small. We also define a generalized operator,

$$\begin{aligned} Q_m^{(n)}(t, z^*) &= \int_0^t \dots \int_0^t \alpha(t-v_1) \dots \alpha(t-v_m)\tilde{z}_{v_{m+1}}^* \\ &\quad \dots \tilde{z}_{v_n}^* \bar{O}^{(n)}(t, v_1, \dots, v_n) dv_1 \dots dv_n. \end{aligned} \quad (7)$$

For $m \neq 0$, $Q_m^{(n)}$ does not contribute directly to \bar{O} but is an auxiliary operator needed to be solved simultaneously. Let $\langle g_k \rangle$ be a mean coupling strength. Up to leading orders $\alpha(t) \sim \langle g_k \rangle^2$, we have, $\tilde{z}_t^* \sim \langle g_k \rangle$, and hence $Q_m^{(n)} \sim \langle g_k \rangle^{n+m+2}$ when using also $\bar{O}^{(n)} \sim \alpha(t)$ [17].

All $Q_m^{(n)}$'s are zero at time $t = 0$. Hence, for sufficiently small t , $Q_m^{(n)} \sim t^n \rightarrow 0$ for a large n . Thus, $Q_m^{(n)}$ has a finite support (i.e. a domain where $Q_m^{(n)}$ takes non-zero values) on the (n, m) -plane which expands with t . More importantly, the infinite series in Eq. (5) is then guaranteed to be convergent at least for small t . Therefore, Eq. (6) can be arbitrarily accurate at a finite N_Q . As t increases especially for the strong coupling regime, the support may expand unboundedly. In practice, we impose the constraint $N_Q \leq \mathcal{N}$ and consider $Q_m^{(n)}$ only up to $n + m \leq \mathcal{N}$ corresponding to order $\langle g_k \rangle^{\mathcal{N}+2}$. Here the higher order terms are neglected.

For simplicity, we consider the environmental noise z_t characterized by the Ornstein-Uhlenbeck noise with the auto-correlation,

$$\alpha(t-s) = \frac{\Gamma\gamma}{2}e^{-\gamma|t-s|}. \quad (8)$$

Taking the time derivative of Eq. (7) and applying the evolution equation of $\bar{O}^{(n)}$ [17], we arrive at our central analytical result after some algebra,

$$\begin{aligned} \dot{Q}_m^{(n)} &= \delta_{n,0}\alpha(0)L + \frac{m}{n'}\alpha(0)\left[L, Q_{m-1}^{(n-1)}\right] + \frac{n-m}{n'}\tilde{z}_t^*\left[L, Q_m^{(n-1)}\right] - (m+1)\gamma Q_m^{(n)} - i\left[H_s, Q_m^{(n)}\right] \\ &\quad - \sum_{k=0}^n \sum_{l=a}^{l_b} \frac{C_l^k C_{n-m-l}^{n-k}}{C_m^n} \left[L^\dagger Q_{k-l}^{(k)}, Q_{m-k+l}^{(n-k)}\right] - (n+1)L^\dagger Q_{m+1}^{(n+1)}, \end{aligned} \quad (9)$$

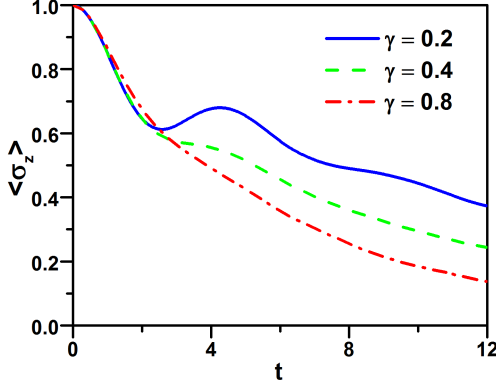


FIG. 1. (color online) Spin state $\langle \sigma_z \rangle$ for various memory parameters: $\gamma = 0.2, 0.4$, and 0.8 . Here, $\omega = 1$, $\Gamma\gamma = 0.2$ and $\mathcal{N} = 100$.

where $n' = \max\{1, n\}$, $l_a = \max\{0, k - m\}$, $l_b = \min\{k, n - m\}$, $Q_m^{(-1)} = Q_{-1}^{(n)} = 0$, and C_l^k is the binomial coefficient. Equations (3), (4), and (9) for $n + m \leq \mathcal{N}$ then constitute a set of coupled SODE's from which $\tilde{\psi}_t(\tilde{z}^*)$ may be obtained.

Results on spin-boson model. – Now we apply our method to a spin-boson model with $H_{\text{sys}} = \frac{\omega}{2}\sigma_z$ and $L = \sigma_x$ [22–24] assuming an initial system state of $\langle \sigma_z \rangle = 1$ with the bath at zero temperature. In the following calculations, all coupling strengths and frequencies are in units of ω . The bath has a memory time $1/\gamma$, with $\gamma = 0.2, 0.4$ or 0.8 , and a coupling constant $\Gamma\gamma = 0.2$ in the strong coupling regime. Each statistical mean involves an ensemble of $N_z = 8000$ of complex colored Gaussian noise z_t obeying the correlation function in Eq. (8). For each realization z_t , we obtain one quantum trajectory $\tilde{\psi}_t(\tilde{z}_t^*)$ by numerically solving the SODE's up to $\mathcal{N} = 100$ terms. The reduced density matrix of the system is recovered by a statistical mean: $\rho_t = \langle |\tilde{\psi}_t(\tilde{z}^*)\rangle\langle \tilde{\psi}_t(\tilde{z}^*)| \rangle$.

Figure 1 shows the evolutions of $\langle \sigma_z \rangle$. For $\gamma = 0.2$ corresponding to a relatively long memory time in our study, an oscillatory behavior superimposed with a non-exponentially decay of $\langle \sigma_z \rangle$ is observed, exemplifying strong non-Markovian effects. The decay behavior becomes more monotonic as γ is increased. At $\gamma = 0.8$, it is essentially exponential early on, demonstrating weak memory effects [22]. In general, exponential decays is ensured when $t \gg 1/\gamma$. As will be explained below, $\langle \sigma_z \rangle$ reported in Fig. 1 admits about 1% error.

For comparison, the result for the most interesting case of $\gamma = 0.2$ is replotted in Fig. 2 and labelled as $\mathcal{N} = 100$. We also plot $\langle \sigma_z \rangle$ calculated similarly using RWA by taking $L = \sigma_-$. RWA is known to be accurate when the system-bath coupling is weak. At strong coupling considered here, we observe that the non-Markovian oscillatory behavior of $\langle \sigma_z \rangle$ is successfully reproduced. However, $\langle \sigma_z \rangle$ drops considerably faster than expected, indicating

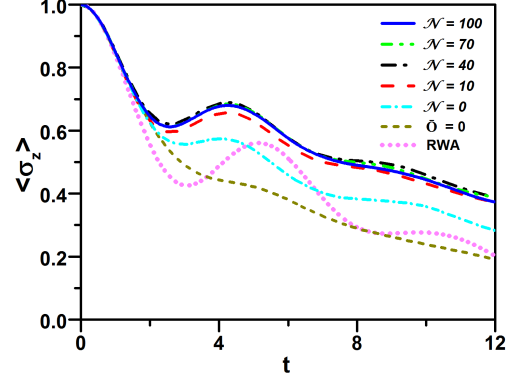


FIG. 2. (color online) Spin state $\langle \sigma_z \rangle$ for $\mathcal{N} = 100, 70, 40, 10$, and 0 , $\bar{O} = 0$, and RWA. Here, $\gamma = 0.2$ and $\Gamma\gamma = 0.2$.

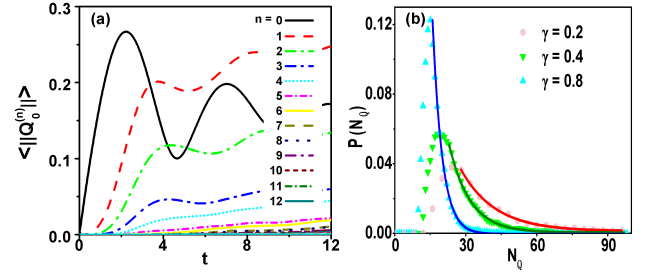


FIG. 3. (color online) (a) Average $\langle \|Q_0^{(n)}\| \rangle$ of the trace norm of perturbative terms $Q_0^{(n)}$ from the simulation in Figure 1 for $\gamma = 0.2$. (b) The probability density $P(N_Q)$ of N_Q at $t = 12$ from the simulations in Figure 1 for $\gamma = 0.2, 0.4$, and 0.8 . Solid lines show fits to exponential distributions for the tails of the distributions.

the reduction of the non-Markovianity due to neglecting the counter-rotating terms [24].

Algorithms and accuracy. – Figure 3 (a) plots the average $\langle \|Q_0^{(n)}\| \rangle = \langle \text{Tr} \sqrt{Q_0^{(n)\dagger} Q_0^{(n)}} \rangle$ of the trace norm of each perturbative term in Eq. (6) for $\gamma = 0.2$. Initial oscillatory behaviors are observed in the four lowest orders and should be responsible for the similar oscillations in $\langle \sigma_z \rangle$. Moreover, note that the low-order terms rise from 0 earlier than the high-order ones. This verifies that the support of $Q_m^{(n)}$ expands gradually from low orders as explained above. For $n \gtrsim 10$, $\langle \|Q_0^{(n)}\| \rangle$ is already close to 0, implying good convergence of the functional expansion. We also observe that $\langle \|Q_0^{(n)}\| \rangle$ tends to become constant at large t . Such saturation is indeed clearly observed for $\gamma = 0.4$ and 0.8 at $t \gg 1/\gamma$, and the saturated value decreases exponentially to 0 with n . For any given realization, $\|Q_0^{(n)}\|$ however persists to fluctuate and arrives only at a dynamic steady state.

To solve the SODE's efficiently, we hence put $N_Q = 1$ initially and increase it adaptively during the time integration with Euler's method and a time step $\Delta t = 0.02$.

Only $Q_m^{(n)}$'s for $n + m \leq N_Q$ are calculated and the rest are approximated by zeros. $Q_m^{(n)}$'s for $n + m = N_Q$ are monitored at every time step. If the magnitude of any of their matrix elements goes beyond a threshold $\epsilon_{\text{thres}} = 10^{-8}$, N_Q is incremented unless it has reached \mathcal{N} , and the last Euler's step is recalculated.

The number of calculated terms N_Q hence indicates the number of non-zero terms in the functional expansion. It depends on both t and z_t^* , and hence admits ensemble fluctuations. Figure 3 (b) plots the probability density $P(N_Q)$ of its final value at $t = 12$ for $N_Q < \mathcal{N}$ from the simulations in Fig. 1. Interestingly, we observe that the distribution is not narrow. The tails fit very well to exponential forms. The average $\langle N_Q \rangle$ increases with the memory time $1/\gamma$. Moreover, it also increases with the coupling constant $\Gamma\gamma$ (results not shown).

To study the importance of individual terms, we have also simulated with $\bar{O} = 0$ (i.e. $\mathcal{N} < 0$), $\mathcal{N} = 0$ and $\mathcal{N} = 10$. The results are shown in Fig. 2. We observe as expected that the decay of $\langle \sigma_z \rangle$ becomes faster and more monotonic when fewer terms are included. Incidentally, the results for $\bar{O} = 0$ and $\mathcal{N} = 0$ for $\gamma = 0.2$ in Fig. 2 resemble respectively the accurate results for $\gamma = 0.8$ and 0.4 in Fig. 1. This suggests that neglecting the non-Markovian terms effectively decreases the bath correlation time. For $\mathcal{N} = 10$, $\langle \sigma_z \rangle$ has nearly converged to the accurate result at $\mathcal{N} = 100$.

Moreover, for $\gamma = 0.2$ and $\mathcal{N} \gtrsim 20$, the solution of the SODE's unexpectedly becomes non-trivial. Once N_Q is constrained at \mathcal{N} and the magnitude of a matrix element of $Q_m^{(n)}$ with $n + m = \mathcal{N}$ exceeds a tolerance $\epsilon_{\text{tol}} = 10^{-4}$, the SODE's eventually become unstable with $Q_m^{(n)}$ at large n and m , diverging smoothly but rapidly with t even at much reduced Δt . The concerned noise realization z_t^* is hence rejected and excluded from all ensemble averages. Allowing rejection, we have also performed simulations at $\mathcal{N} = 40$ and 70 and the results are plotted in Fig. 2. The rejection rates for $\mathcal{N} = 40, 70$, and 100 are $R = 11\%$, 6.6% and 5.4% , respectively. Due to the exponential distribution of N_Q , R is expected to decrease exponentially against \mathcal{N} . We find that the rejected noise realizations z_t^* in general are those with large magnitudes. The rejection induces errors associated with an ensemble bias which decreases with \mathcal{N} . Again, the result for $\mathcal{N} = 70$ has nearly converged to our most accurate result at $\mathcal{N} = 100$. For $\gamma = 0.4$ and 0.8 as shown in Fig. 1, $\langle N_Q \rangle$ is much smaller and thus noise rejection events become rare.

Since the SODE's are exact, the errors occurring in our algorithm can be fully analyzed. The r.m.s. error of $\langle \sigma_z \rangle$ can be approximated by $\sqrt{\mathcal{E}_{Nz}^2 + \mathcal{E}_{\Delta t}^2 + \mathcal{E}_{\mathcal{N}}^2}$. Here, $\mathcal{E}_{Nz} \sim 1/\sqrt{N_z}$ denotes the ensemble sampling error. For all calculations reported in Fig. 1, we find $\mathcal{E}_{Nz} \simeq 0.004$ after averaging over time. The time discretization error $\mathcal{E}_{\Delta t}$ is found to be about 0.001 from simulations with

identical noise but different Δt . Also, $\mathcal{E}_{\mathcal{N}}$ is due to including at most $\mathcal{N} = 100$ perturbative terms. For $\gamma = 0.4$ and 0.8 , $\mathcal{E}_{\mathcal{N}} \simeq 0$ because higher order terms are vanishingly small. For $\gamma = 0.2$, we find $\mathcal{E}_{\mathcal{N}} \simeq 0.002$ from comparing results at $\mathcal{N} = 70$ and 100 with identical noise. Finally, $\langle \sigma_z \rangle$ admits about 1% error in all three cases. The simulations for $\gamma = 0.2, 0.4$ and 0.8 take about 36, 10, and 2 days respectively to execute on a Intel core-i7 CPU core. Indeed, QSD approaches are fully parallelizable. The accuracy for $\gamma = 0.4$ and 0.8 can be further improved substantially by increasing N_z . More challenging is the $\gamma = 0.2$ case since one must also reduce $\mathcal{E}_{\mathcal{N}}$ by increasing \mathcal{N} . This leads to much more intensive computations. Noting that the program run-time is of the order $N_z \mathcal{N}^4 / \Delta t$. Minimizing $\mathcal{E}_{\mathcal{N}}$ and \mathcal{E}_{Nz} simultaneously to produce accurate results will be critical and challenging when pushing to even stronger couplings.

In conclusion, we have developed a high-order non-Markovian QSD approach for open quantum systems based on a set of coupled SODE's which can be efficiently implemented in numerical simulations. As an important example, our method is applied to a spin-boson model with a Lorentzian bath spectrum at zero temperature in the strong coupling regime. Note that a generalization to the finite temperature case is straightforward [25]. In particular, for this spin-boson model, the finite-temperature non-Markovian QSD equation actually takes the exact same form as the zero-temperature one. Numerically, an extension to general interaction spectra may also be possible by including coupled equations for new operators analogous to $Q_m^{(n)}$ in Eq. (7) but with some α 's replaced by their derivatives. Our numerical simulations of the spin-boson model have shined a new light into the spin dynamics without the RWA. It is shown that even though the RWA may successfully reproduce non-Markovian spin state transient oscillations, it cannot accurately capture the bath memory effects.

Note added: Close to the completion of this work, we become aware of a different kind of numerically exact hierarchical equations by W. Strunz and coworkers [26].

This work is supported by the National Natural Science Foundation of China Grant No. 91121015, the National Basic Research Program of China Grant No. 2014CB921401, the NSAF Grant No. U1330201, Hong Kong GRF Grant No. 501213, and the China Postdoctoral Science Foundation Grant No. 2012M520146. TY is grateful to Prof. J. Q. You for the hospitality during his visit to the CSRC, Beijing.

* Z.Z.L and C.T.Y contributed equally to this work.

[1] M. A. Nielsen and I. L. Chuang, Quantum Computation and Quantum Information (Cambridge University, Cambridge, England, 2000).

- [2] M. O. Scully and M. S. Zubairy, *Quantum Optics* (Cambridge University Press, Cambridge, England, 1997).
- [3] H. P. Breuer and F. Petruccione, *Theory of Open Quantum Systems* (Oxford University, New York, 2002).
- [4] S. John and J. Wang, Phys. Rev. Lett. **64**, 2418 (1990); S. John and T. Quang, Phys. Rev. A **52**, 4083 (1995); O. Toader, T. Chan, and S. John, Phys. Rev. Lett. **92**, 043905 (2004).
- [5] C. Emary and T. Brandes, Phys. Rev. Lett. **90**, 044101 (2003).
- [6] S. D. Liberato, C. Ciuti, and I. Carusotto, Phys. Rev. Lett. **98**, 103602 (2007).
- [7] A. G. Kofman and G. Kurizki, Phys. Rev. Lett. **93**, 130406 (2004).
- [8] H. Zheng, S. Y. Zhu, and M. S. Zubairy, Phys. Rev. Lett. **101**, 200404 (2008).
- [9] X. Cao, J. Q. You, H. Zheng, A. G. Kofman, and F. Nori, Phys. Rev. A **82**, 022119 (2010).
- [10] S. Agarwal, S. M. H. Rafsanjani, and J. H. Eberly, Phys. Rev. A **85**, 043815 (2012).
- [11] A. T. Sornborger, A. N. Cleland, and M. R. Geller, Phys. Rev. A **70**, 052315 (2004).
- [12] T. Werlang, A. V. Dodonov, E. I. Duzzioni, and C. J. Villas-Bôas, Phys. Rev. A **78**, 053805 (2008).
- [13] B. L. Hu, J. P. Paz, and Y. Zhang, Phys. Rev. D **45**, 2843 (1992).
- [14] L. Diósi and W. T. Strunz, Phys. Lett. A **235**, 569 (1997).
- [15] L. Diósi, N. Gisin, and W. T. Strunz, Phys. Rev. A **58**, 1699 (1998).
- [16] W. T. Strunz, L. Diósi, and N. Gisin, Phys. Rev. Lett. **82**, 1801 (1999).
- [17] T. Yu, L. Diósi, N. Gisin, and W. T. Strunz, Phys. Rev. A **60**, 91 (1999).
- [18] W. T. Strunz and T. Yu, Phys. Rev. A **69**, 052115 (2004).
- [19] J. Jing and T. Yu, Phys. Rev. Lett. **105**, 240403 (2010).
- [20] J. Jing, X. Zhao, J. Q. You, and T. Yu, Phys. Rev. A **85**, 042106 (2012).
- [21] J. Jing, X. Zhao, J. Q. You, W.T. Strunz, and T. Yu, Phys. Rev. A **88**, 052122 (2013).
- [22] D. Lacroix, Phys. Rev. E **77**, 041126 (2008).
- [23] G. Clos and H. P. Breuer, Phys. Rev. A **86**, 012115 (2012).
- [24] H. Mäkelä and M. Möttönen, Phys. Rev. A **88**, 052111 (2013).
- [25] T. Yu, Phys. Rev. A **69**, 062107 (2004).
- [26] D. Süß, A. Eisfeld, and W. T. Strunz, arXiv:1402.4647.